Toward Origami-Inspired In Vitro Cardiac Tissue Models

ACS Biomaterials SCIENCE & ENGINEERING

pubs.acs.org/journal/abseba
Article

Toward Origami-Inspired In Vitro Cardiac Tissue Models

Antonio Sileo, Federica Montrone, Adelin Rouchon, Donata Trueb, Jasmin Selvi, Moritz Schmid, Julian Graef, Fabian Züger, Gianpaolo Serino, Diana Massai, Nunzia Di Maggio, Gabriela Melo Rodriguez, Joachim Köser, Joachim Schoelkopf, Andrea Banfi, Anna Marsano,*,▽ and Maurizio Gullo▽

Cite This: ACS Biomater. Sci. Eng. 2025, 11, 1583−1597
Read Online

ACCESS | Metrics & More | Article Recommendations | Supporting Information

ABSTRACT: The advancement of *in vitro* engineered cardiac tissue-based patches is paramount for providing viable solutions for restoring cardiac function through *in vivo* implantation. Numerous techniques described in the literature aim to provide diverse mechanical and topographical cues simultaneously, fostering enhanced *in vitro* cardiac maturation and functionality. Among these, cellulose paper-based scaffolds have gained attention owing to their inherent benefits, such as biocompatibility and ease of chemical and physical modification. This study introduces a novel approach of utilizing customized paper-based scaffolds as cell culture substrates, facilitating both the formation and manipulation of cell constructs while promoting mechanical contraction. Here, we investigated two methodologies to foster mechanical contractions of paper-based constructs: the incorporation of micropatterns on paper to dictate cell orientation and macropattern created by the origami-folded paper. Both approaches provide mechanical support and foster cardiac functionality. However, while micropatterning does not significantly improve the functional parameters, a macropattern created by origami folding proves to be essential in facilitating contraction of the paper-based cardiac constructs. Furthermore, we provide proof of principle for the combination with a layer of physiologically differentiated microvascular networks. This approach holds great promise for the development of structurally organized contractile cardiac tissues with the possibility of creating multistrata of cardiac and vascular layers to promote *in vivo* cell survival and function beyond what is typically achieved in conventional cell culture.

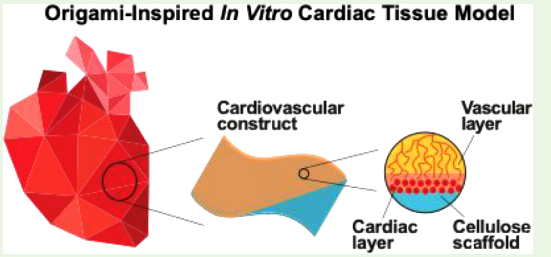

KEYWORDS: *cardiac tissue engineering, in vitro models, hydrogel, cell alignment, Miura-ori included pattern, origami-folded paper, vascular layer*

1. INTRODUCTION

In vitro engineered cardiac tissues (ECTs) hold considerable promise as cell-based patch solutions for restoring cardiac function in infarcted myocardial regions. Among various patch-based approaches, engineering cell sheet-based cardiac patches has emerged as a promising strategy, facilitating the creation of well-aligned and interconnected cardiomyocytes.[1−4]

The alignment of cardiomyocytes within the native myocardium is crucial for proper electrical signal propagation and synchronized contraction.[4,5] Techniques such as electrospinning, microfabrication, and microcontact printing have been pivotal in creating patterned scaffolds that direct cell growth, mimicking this alignment. Numerous studies have highlighted the benefits of scaffolds characterized by cell alignment cues, resulting in improved sarcomere organization, intercellular communication, and cell elongation.[4,6−8] Advances in the biofabrication of biomimetic cardiac patches showed that micropatterned hydrogels, featuring single lanes or bridged lanes, have been instrumental in promoting cardiomyocyte alignment, maturation, and synchronous beating.[9,10]

The success of cell-based patches relies on appropriate structural, physical, and biocompatible cell culture substrates capable of supporting the growth of multiple cell layers, ultimately forming functional 3D tissue constructs.[11,12] Among the various prerequisites, cardiac patches should have appropriate physical properties in terms of mechanical competence to support handling and cell maturation, and the biological ones include cell adherence, biocompatibility, and biodegradation. Currently adopted strategies are the production of cell sheets, which can be easily detached and transported, thanks to temperature-sensitive culture plate coatings[11,13] as well as electrospun nanofiber patches presenting extracellular matrix−like structural features, such as mechanical support.[14]

Received: August 30, 2024
Revised: January 16, 2025
Accepted: January 17, 2025
Published: February 20, 2025

The combination of multiple mechanical, topographical, and biological cues such as proper stiffness, anisotropy, and cell−cell contact is necessary to enhance *in vitro* cardiac maturation and organization.[15] The variation in substrate stiffness, ranging from 10 to 20 kPa within the physiological range[16−18] and up to 123 kPa for fibrotic tissue, can impact the cell morphology, behavior, and differentiation.[20] Polyacrylamide hydrogel matrices with ranges of stiffness corresponding to embryonic (12 kPa), adult (30 kPa), or fibrotic (123 kPa) cardiac tissues showed that soft stiffness substrates promoted a highly organized sarcomeric structure, while a stiff matrix impaired contractile function with disorganized sarcomeres.[17] An increased cell spread area, binucleation, and maximal calcium intensities were observed in human embryonic stem cell-derived cardiomyocytes cultured on substrates with 21 kPa stiffness, in comparison to softer and stiffer substrates.[15] Paper-based products attracted increasing attention in healthcare, pharmaceutical, and biomedical research, thanks to their promising properties such as biocompatibility, ease of chemical and physical modification, cost efficiency, eco-friendliness, and scalability.[21] Paper has been recently applied as an alternative substrate for cell culture,[22] although coating or printing with cell adhesion promoters is necessary since paper itself lacks cell adhesion moieties.[23] Researchers have explored various applications of paper in cell culture, such as using paper coated with the polydimethylsiloxane (PDMS) elastomer for the proliferation and differentiation of human-induced pluripotent stem cells (hiPSCs) into functional beating cardiac tissues[24] or utilizing multilayered stacks of paper sheets made of cardiac cells embedded in hydrogel matrices to create a 3D cardiac ischemic tissue model.[25] Moreover, paper-based scaffolds have been employed for the generation and analysis of engineered heart valve tissues by embedding cells in thick collagen matrix stacks between paper layers to mimic the thickness of native valve leaflets.[26] However, modifying the stiffness of these paper-based scaffolds to facilitate cardiac maturation and contraction poses challenges.

To address this challenge, we proposed the use of hydrogel-based micropatterning or macrofolding to promote the contraction of cardiac constructs while maintaining mechanical handling. In particular, we introduced the unique use of origami techniques to fold paper-based scaffolds into a Miura-ori-included pattern, enabling in-plane contraction of cardiac tissues.

A critical aspect for successful patch implantation is the presence of a blood vessel network. Efficient vascularization is not only necessary to ensure cell survival and maturation *in vivo* of ECTs[11] but also contributes to cardiomyocyte growth and cardiac repair independently of its role in supplying oxygen and nutrients, i.e., the so-called angiocrine function.[11] Therefore, it is important to incorporate a vascular component in a physiological model of *in vitro* ECT.

Here, we developed a manufacturing method for obtaining contractile and structurally organized cardiac monolayers, including a self-assembled microvascular network, using Miura-ori papers as cell culture substrates. We assessed the importance of combining mechanical and environmental cues to achieve the contractility and organization of cardiac cells. In addition, we investigated the directional growth and organization of cardiomyocytes through physical alignment cues in two-dimensional (2D) cultures and on paper-based scaffolds. The included Miura-ori patterns proved to be fundamental for achieving cell contractility.

2. MATERIALS AND METHODS

2.1. Production of Gelatin Hydrogel and Characterization.

2.1.1. Gelatin Preparation. The formulation method of the gelatin hydrogel is based on previous work where the details on gelation dynamics and rheological properties are presented.[27] In brief, gelatin is a biopolymer used as a substrate for cell attachment, allowing the cell to engraft on a substrate with a stiffness that resembles the cardiac tissue more than cell culture plastic does. In this study, type A gelatin from porcine skin (Sigma-Aldrich, USA) was adopted. It was diluted in Dulbecco's phosphate-buffered saline (DPBS, Sigma-Aldrich, USA) and enzymatically cross-linked at the physiological temperature (37 °C) with transglutaminase (TG, Sigma-Aldrich, USA). This type of gelation process is more reliable in terms of biocompatibility and stability of the gel as well.[28] Enzymatic gelation represents a safer alternative to the usual glutaraldehyde covalent cross-linking, consequently avoiding the risk of toxic leftover residuals from the gelation process.[29] The TG catalyzes the formation of covalent bonds, providing thermal stability and insolubility in water.[30] DPBS was employed because it maintains the pH in a physiological range of about 7.4. The concentration of gelatin powder diluted in DPBS affects the viscosity and the stiffness of the hydrogel, while the concentrations of TG diluted in DPBS (50 and 100 mg/mL) play a role in the gelation rate and possibly also in stiffness.

2.1.2. Nanoindentation Test and Selection of Gelatin Concentration. The maturation of cardiomyocytes can be improved by using substrates with stiffness values similar to those of native cardiac tissue. In this perspective, different gelatin compositions (4, 6, 9, and 12% w/v) enzymatically gelled with two different enzyme concentrations (50 or 100 mg/mL) were prepared and mechanically characterized by nanoindentation.

Nanoindentation tests were performed at physiological temperature (37 °C) and in phosphate-buffered saline (PBS, Sigma-Aldrich, USA) solution in order to mimic the native tissue conditions, using a Piuma nanoindenter (Optics11, NL) and controlling the indentation depth (tip radius (r) = 49.5 μm; cantilever stiffness (K_{tip}) = 0.48 N/m; indentation depth (δ) = 5 μm for 4% and 6% w/v gelatin samples, and δ = 3.5 μm for 9 and 12% w/v gelatin samples). An area of 3600 μm^2 was explored for each sample, setting a scanning step size of 150 μm. To extract the mechanical properties of the samples, the experimental curves were fitted through the Hertz model during the first part of the loading phase of the nanoindentation process. A Poisson's ratio (υ) of 0.5 was assumed. According to the Hertz contact theory, the applied load (P) can be expressed as

$$P = \frac{4}{3}\cdot E^*\cdot\sqrt{r}\cdot\delta^{3/2} \tag{1.1}$$

where E^* is the effective modulus, given by

$$\frac{1}{E^*} = \frac{(1-\upsilon^2)}{E_{sample}} + \frac{(1-\upsilon'^2)}{E_{tip}} \tag{1.2}$$

where E_{sample} is the elastic modulus of the sample and υ' is the Poisson's ratio of the indenter. Assuming that the stiffness of the nanoindenter tip is infinitely higher than the sample ($E_{tip} \gg E_{sample}$), the elastic modulus of the sample can be obtained as

$$E_{sample} \sim \frac{3\cdot(1-\upsilon^2)\cdot P}{4\cdot\sqrt{r}\cdot\delta^{3/2}} \tag{1.3}$$

To select a suitable gelatin composition, the mechanical characterization was complemented by a cell culture test for investigating the behavior of cardiac cells with respect to different compositions. For this purpose, the different gelatin solutions enzymatically gelled with two different concentrations of enzymes were poured (192 μL) in tissue culture plates, and neonatal rat cardiac cells (NRCCs) (~70% cardiomyocytes and ~30% fibroblasts) were seeded on top (6×10^5 cells/cm^2) and cultivated for 6 days in static conditions in a standard incubator (37 °C, 5% CO_2). Functional analysis on the neonatal rat cardiomyocytes (NRCMs) was performed at the end of the culture by using carbon rod electrodes placed at a distance of 1.1 cm.

https://doi.org/10.1021/acsbiomaterials.4c01594
ACS Biomater. Sci. Eng. 2025, 11, 1583−1597

2.2. Production of the PDMS Pattern. Line patterns with lateral dimensions of 5 to 100 μm and a depth of 40 μm were produced by UV contact photolithography using SU8 series negative photoresists (MuWells Inc., San Diego, USA). The micropatterned silicon wafer was used as received to create PDMS (Sylgard 184, Dow Corning Co., USA) replicas, and the dimensions were verified by confocal laser scanning microscopy (Olympus LEXT OLS3000; Olympus Deutschland GmbH, Hamburg, Germany) and scanning electron microscopy (Zeiss Supra 40VP, Carl Zeiss AG, Oberkochen, Germany).

2.3. Production of Paper. The manufacturing of the paper-based supports and Miura-ori pattern folding is described elsewhere.[31] In brief, cotton linter fiber–based papers with 40 g/m^2 thickness have been manufactured with a Rapid-Köthen sheet former and sterilized by autoclaving. Mechanical properties of the cotton linters are strain at break 1.3 ± 0.1%, tensile strength 4.7 MPa, and E modulus 0.8 ± 0.1 GPa.[31] The Miura-ori pattern was first embossed into a pair of polymeric foils by means of custom-made polymeric stamps. The cellulose paper sheet was then sandwiched between the two unfolded foils, and the Miura-ori pattern was transferred by folding the stack. In order to stabilize the papers for prolonged cell culture, they were wetted with 12% w/v gelatin containing 100 mg/mL TG and cross-linked for 1 h in a cell culture incubator at 37 °C and 5% CO_2.

2.4. Cardiomyocyte and Fibroblast Isolation. NRCCs were isolated from 2 to 3-day-old Sprague–Dawley rats as previously described.[32] Briefly, rat ventricles were cut into small pieces and digested overnight in 0.06% (w/v) trypsin solution (trypsin from bovine pancreas, Sigma-Aldrich, USA) at 4 °C with continuous shaking at 50–60 oscillations per minute. Five continuous 4-min cycles of 0.1% w/v collagenase solution treatment were used to continue digestion of the minced tissues (type 2 collagenase, Worthington-Biochem, USA). To allow neonatal rat fibroblast (NRFB) attachment and enrich the cell population for NRCMs, isolated cardiac cells were preplated in culture flasks for 45 min at 37 °C and 5% CO_2. The enriched cardiac population (>70% cardiomyocytes) was seeded at a density of 6 × 10^4 cells/cm^2 and cultured for 48 h, before starting the experiments, in high glucose (HG) Dulbecco's Modified Eagle's Medium (DMEM, Sigma-Aldrich, USA), supplemented with 1% v/v HEPES buffer (Sigma-Aldrich, USA), 1% v/v penicillin/streptomycin (Sigma-Aldrich, USA), 1% v/v L-glutamine (Sigma-Aldrich, USA), and 10% v/v fetal bovine serum (FBS, Sigma-Aldrich, USA) (seeding medium).

For pattern alignment studies, embryo rat fibroblasts (Rat2, *Rattus norvegicus*, ATCC-CRL-1764) were used and expanded in HG DMEM (Sigma-Aldrich, USA) supplemented with 10% (v/v) FBS (Sigma-Aldrich, USA) and 1% (v/v) penicillin/streptomycin (Sigma-Aldrich, USA).

2.5. HUVEC Culture. Pooled donor human umbilical vein endothelial cells (HUVECs) were purchased from PromoCell (Heidelberg, Germany, C-12203) and expanded at 37 °C with 5% CO_2. HUVECs were cultured in Endothelial Cell Growth Medium-2 (EGM-2) supplemented with 2% FCS, 5 ng/mL EGF, 10 ng/mL bFGF, 20 ng/mL IGF, 0.5 ng/mL VEGF165, 1 μg/mL ascorbic acid, 22.5 μg/mL heparin, 0.2 μg/mL hydrocortisone (PromoCell, Heidelberg, Germany, C-22011), and 1% penicillin/streptomycin (P/S) (Gibco, Thermo Fisher Scientific, Waltham, Massachusetts, USA) according to the manufacturer's instructions. For all experiments, HUVECs were used between passages 4 and 5.

2.6. ASC Isolation and Culture. Samples of human adipose tissue were collected either as liposuction, lipoaspirate, or as excision material obtained during routine surgical procedures at the Department of Plastic Surgery of the Basel University Hospital. Informed consent was obtained preoperatively, and the protocol was approved by the local ethical committee (Ethikkommission beider Basel [EKKB], ref. 78/07). Stromal vascular fraction (SVF) cells were isolated after enzymatic digestion of adipose tissue with 0.15% collagenase type II (Worthington, Lakewood, NY) and $CaCl_2$ (250 mM; Linza, Basel, Switzerland) and centrifugation. SVF cells were finally suspended in complete medium (CM), consisting of α-minimal essential medium (MEM) (Gibco, Thermo Fisher Scientific, Waltham, Massachusetts, USA) supplemented with 10% fetal bovine serum (FBS) (HyClone, South Logan, Utah, USA), 1% HEPES (Gibco, Thermo Fisher Scientific, Waltham, Massachusetts, USA), 1% sodium pyruvate (Gibco, Thermo Fisher Scientific, Waltham, Massachusetts, USA), 1% glutamine solutions, and 1% P/S (Gibco, Thermo Fisher Scientific, Waltham, Massachusetts, USA) and filtered through a 100-μm strainer. To ensure adipose-derived stromal cell (ASC) selection, SVF cells were seeded onto tissue culture plates at a density of 10^4 cells per cm^2 for monolayer expansion and cultured in NRCM supplemented with 5 ng/mL fibroblast growth factor-2 (FGF-2) (R&D Systems, Minneapolis, Minnesota, USA) for 7–8 days at 37 °C and 5% CO_2 until subconfluence. For all experiments, ASCs were expanded in NRCM supplemented with 5 ng/mL FGF-2 and were used at passage 1.

2.7. Pattern Generation and Cell Culture. *2.7.1. Pattern Generation on the Gelatin Substrate.* In order to assess the effects of the gelatin substrate and cell alignment (made by using a patterned PDMS membrane with 25 μm width) on cardiac functionality, NRCCs were cultured at a density of 10^5 cells/cm^2 on a tissue culture plate without (TCP − P-control) or with 12% w/v gelatin substrate decorated with (gel + P) or without (gel − P) a pattern for 6 days.

The height of the substrate of gelatin 12% w/v, cross-linked through TG (100 mg/mL), was chosen to have a limited thickness of 200 μm, useful for high magnification microscopes. The PDMS stamps with patterned or smooth (for the control) surface were placed on top of the gelatin, and the samples were stored in the incubator at 37 °C and allowed to cross-link overnight. After the cross-linking, the PDMS stamps were removed from the gelatin in which the negative mold of the patterned surface of the PDMS membrane remained. Then, the pH of patterned gelatin samples was equilibrated for at least 1 h in HG DMEM supplemented with 10% v/v FBS, 1% v/v PS, 1% v/v HEPES, and 1% v/v L-Glu. The exhausted culture media was then removed, and the NRCCs were seeded drop by drop on top of the gelatin. In the end, after another hour, which allowed the cells to adhere on the gelatin, fresh DMEM was added.

After 1 day of culture, the culture media was replaced with low glucose (LG) DMEM (Sigma-Aldrich, USA) supplemented with 1% v/v FBS, 1% v/v PS, 1% v/v HEPES, and 1% v/v L-Glu in order to limit the proliferation of fibroblasts, which is favored with a high concentration of FBS and glucose. The culture media was changed every 2 days.

2.7.2. Pattern Generation on the Paper-Based Gelatin Substrate. Following the same protocol described earlier, NRCCs were seeded at a density of 10^5 cells/cm^2 on rectangular cellulose paper (paper size: 0.5 cm × 1 cm, paper density: 40 g/m^2). Two different surfaces were used: a patterned surface (gel + P) and a smooth surface (gel − P), both coated with 12% w/v gelatin. Additionally, to examine the influence of the paper's fiber orientation on cell movement, cells were also cultured on a paper with oriented fibers in the presence of a smooth 12% w/v gelatin surface. After 1 day of culture, the high glucose (4500 mg/mL) DMEM used for cell seeding was replaced with low glucose (1000 mg/mL) DMEM supplemented with 1% v/v FBS, 1% v/v PS, 1% v/v HEPES, and 1% v/v L-Glu. The culture media was changed every 2 days.

2.7.3. Cardiac Cells Cultured in Hydrogel-Based Cardiac Constructs on Unfolded and Miura-Ori Paper. 2.7.3.1. Generation of Hydrogel-Based Cardiac Constructs. NRCCs were embedded in hydrogel-based cardiac constructs as previously described.[33] Briefly, hydrogel-based cardiac constructs were generated by seeding NRCCs in a 50 μL fibrin gel solution (25 mg/mL fibrinogen, 5 U/mL thrombin, 4.4 mM $CaCl_2$, and 0.4 mg/mL tranexamic-acid, Sigma-Aldrich, USA) at the density of 20 × 10^6 cells/mL corresponding to 1 × 10^6 cells. Cardiac constructs were incubated for 20 min at 37 °C and 5% CO_2 to allow complete polymerization of the fibrin gels.

2.7.3.2. Culture of Hydrogel-Based Cardiac Constructs on Unfolded and Miura-Ori Paper. The paper was used as a culture support for hydrogel-based cardiac constructs. The unfolded and Miura-ori papers were stabilized with gelatin, as previously described in Section 2.3. Cells were then seeded on top of Miura-ori and unfolded papers prior to embedding the cardiac construct into a hydrogel. The cardiac constructs were generated by directly casting the cell-based fibrin gel on the unfolded and Miura-ori gelatin–stabilized papers. Cardiac constructs were incubated for 20 min at 37 °C and 5% CO_2 to allow complete polymerization of the fibrin gels. All cardiac constructs were cultured for 7 days (37 °C, 95% humidity, and 5% CO_2) with

https://doi.org/10.1021/acsbiomaterials.4c01594
ACS Biomater. Sci. Eng. 2025, 11, 1583–1597

standard culture medium. Tranexamic acid was supplemented to the culture medium every day at a concentration of 0.4 mg/mL to reduce fibrin gel degradation.[34] After 7 days of culture, functionality analysis under external electrical pacing was performed on cardiac constructs in order to evaluate the biological response.

2.8. Combination of a Vascular Layer with a Paper-Based Cardiac Construct. *2.8.1. Fibrin Hydrogel Preparation for the Vascular Layer.* Fibrin matrices were prepared by mixing 10 mg/mL of human fibrinogen (plasminogen-, von Willebrand factor-, and fibronectin-depleted; Milan Analytica AG, Rheinfelden, Switzerland), 3 U/mL of factor XIIIa (CSL Behring, King of Prussia, Pennsylvania, USA), and 3 U/mL of thrombin (Sigma-Aldrich, St. Louis, Missouri, USA) with 2.5 mM Ca^{2+} in 4-(2-hydroxyethyl)-1-piperazineethanesulfonic acid (HEPES) (Lonza, Basel, Switzerland) with 100 ng/mL of recombinant VEGF-A164 protein, engineered with the transglutaminase substrate octapeptide α2PI1−8 (TG-VEGF),[35] to allow cross-linking into fibrin hydrogels at the indicated concentrations.

2.8.2. 3D Coculture of the Vascular Layer. HUVEC and ASC cocultures were performed with a final density of 5×10^6 cells/mL at a ratio of 1:1. Gel polymerization was achieved in cell culture incubators at 37 °C for 10 min in a 12-well chamber (Ibidi, Gräfelfing, Germany, 81201). Fibrin hydrogels were cultured with the EGM-2 medium, and the medium was refreshed every 2 or 3 days. For experiments with paper-based constructs, the paper was stabilized with gelatin, as previously described in Section 2.3.

2.8.3. Effects of Different Culture Media on 2D Cardiac Cells. NRCCs were isolated as described in Section 2.4. Cells were seeded at a density of 6×10^4 cells/cm^2 corresponding to 2.5×10^5 cells per μ-dish 35 mm chamber (Ibidi GmbH, Germany) using 0.5 mL high glucose DMEM (Sigma-Aldrich, United States), supplemented with 1% HEPES buffer (Sigma-Aldrich, United States), 1% penicillin/streptomycin (Sigma-Aldrich, United States), 1% L-glutamine (Sigma-Aldrich, United States), and 10% FBS (Sigma-Aldrich, United States). From the following day, the medium was changed every 3 days either with 2.5 mL of low glucose (LG) DMEM (Sigma-Aldrich, United States), supplemented with 1% HEPES buffer (Sigma-Aldrich, United States), 1% penicillin/streptomycin (Sigma-Aldrich, United States), 1% L-glutamine (Sigma-Aldrich, United States), and 1% FBS (Sigma-Aldrich, United States) or with 2.5 mL of EGM-2 medium.

After 7 days of culture, cardiac maturation was assessed by immunofluorescence staining for sarcomeric α-actinin and connexin-43 (Cx-43).

2.8.4. Combination of a Vascular Layer with a Paper-Based Cardiac Construct. Fibrin gels of 20 μL for the vascular layer were prepared as described in Section 2.8.2, while fibrin gels of 35 μL for the cardiac layer were prepared as described in Section 2.7.3.1. For the experiment without paper, the cardiac layer was cast in a 12-well chamber (Ibidi GmbH, Germany) and the vascular layer was subsequently cast on top of it. Gel polymerization was achieved in cell culture incubators at 37 °C for 20 min. As control, 55 μL of the cardiac layer alone was cast and cultured. Fibrin hydrogels were cultured with EGM-2 medium + 10% FBS, and the medium was refreshed every day. Tranexamic acid was supplemented to the culture medium every day at a concentration of 0.4 mg/mL to reduce fibrin gel degradation. For experiments with unfolded gelatin-stabilized papers, 100% cotton linters paper was used at the bottom of the 12-well chamber as support for the combination of the vascular and cardiac layer. As control, 55 μL of the cardiac layer alone was cast and cultured on unfolded gelatin-stabilized papers. After 7 days of culture, functional analyses under external electrical pacing were performed in order to evaluate the biological response.

2.9. Immunofluorescence Staining. To investigate cardiac maturation at the end of the culture, immunofluorescence analysis was performed. Cells were washed with phosphate-buffered saline (PBS, Sigma-Aldrich, USA) and fixed using 4% (w/v) PFA (Sigma-Aldrich, USA) for 15 min. Afterward, the immunostaining was executed following a standard protocol. For the unfolded and the Miura-ori paper staining, sections of 10 μm in thickness were cut with a cryostat (Leica Biosystem CM1950, Leica Biosystem, Germany) and stained according to a standard protocol. In detail, cells were washed 2 times with PBS (Sigma-Aldrich, USA), and successively, they were incubated for 1 h at room temperature in 5% v/v normal goat serum (Sigma-Aldrich, USA) with 0.25% v/v Triton 100× (Sigma-Aldrich, USA) in DPBS (Sigma-Aldrich, USA). After washing 2 times with DPBS, cells were incubated for 1 h in the dark with the mouse monoclonal IgG2b Anti-Cardiac Troponin T (Abcam, UK) primary antibody. Cells were again washed 2 times with DPBS and consequently incubated in the dark for 30 min with fluorescently labeled Alexa 488-phalloidin to stain F-actin (Invitrogen, Thermo Fisher Scientific, USA) and fluorescently labeled Alexa 647 antimouse secondary antibody (Life Technologies, Thermo Fisher Scientific, USA). Nuclei were stained using 4′,6-diamidino-2-phenylindole (DAPI, Invitrogen, Thermo Fisher Scientific, USA) at 1:40 for 15 min. Incubations were performed at room temperature, and antibodies were diluted in DPBS 1× with 0.1% w/v bovine serum albumin (BSA, Sigma-Aldrich, USA). Primary and secondary antibody dilution was 1:200. Representative images of different areas of each sample were acquired using 10× and 40× objective lenses on a Nikon-CSU1 spinning-disk confocal microscope (Nikon, Japan) and subsequently analyzed by using ImageJ software (NIH, USA).

On the ultrastructural level, cell elongation is reflected by the orientation of cellular actin filaments.[36] Thus, for quantification of the cell alignment, the orientation of the cellular actin filaments can be employed. Following formalin fixation and membrane permeabilization with 0.1% v/v Triton X-100 in DPBS, actin filaments of cells grown on patterned substrates were stained with phalloidin−tetramethylrhodamine B (Merck) and DAPI. Images were obtained by employing an Olympus FV1000 confocal fluorescence microscope.

For immunofluorescence staining of the vascular layer and the combination of the vascular layer with a paper-based cardiac construct, fibrin hydrogels were fixed with 1% PFA (Sigma-Aldrich, St. Louis, Missouri, USA); washed overday prior to an overnight blocking in PBS (Gibco, Thermo Fisher Scientific, Waltham, Massachusetts, USA), 2% donkey serum, and 0.5% BSA (Lubio Science, Lucerne, Switzerland); and then washed again overday. Afterward, the following primary antibodies were incubated overnight: polyclonal rabbit anti-laminin (Abcam, Cambridge, UK, 11575) at 1:200 and polyclonal goat anti-podocalyxin (R&D System Minneapolis, Minnesota, USA, AF1658) at 1:100. Gels were washed overday both before and after incubation with fluorescently labeled secondary antibodies overnight (Invitrogen, Thermo Fisher Scientific, Waltham, Massachusetts, USA) at 1:200. Nuclei were labeled with DAPI at 0.4 μg/mL (Sigma-Aldrich, St. Louis, Missouri, USA, D9542). All steps were performed at 4 °C on a shaker. Representative images were acquired with a 40× objectives on a Carl Zeiss LSM710 3-laser scanning confocal microscope (Carl Zeiss, Oberkochen, Germany).

2.10. Image Analysis. The immunofluorescence images were postprocessed through ImageJ (version 1.54f) using the Directionality plugin to quantify the directionality of the cells. In the patterned samples, the z-stacks of the images were divided into 2 parts: the first 5 μm of the bottom of the sample (where the cells were aligned in the channels) and the top of the sample (after 40 μm) where the pattern should no longer be present. The reference system was set so that the *X*-axis was parallel to the pattern direction. The plugin generated normalized histograms revealing the number of cells present between −90 and +90° with a bin size of 1° using the Fourier spectrum analysis applied to each image.

The numbers of NRCMs and NRFBs were defined by counting the number of nuclei positive and negative for troponin-T, respectively. All the acquired images were then processed with the threshold technique "Li dark method" to segment troponin-T-positive entities. With these techniques, the percentage of area positive for troponin-T normalized by the number of cardiomyocytes was quantified.[33,37−40]

Vascular analyses were performed on immunofluorescence images. All images used for analysis were taken with a Spinning Disc Confocal Nikon CSU-W1 (Nikon, Tokyo, Japan). Prior to analysis, all selected z-stacks were reduced to maximum intensity projection and the laminin$^+$/podocalyxin$^+$ double-positive structures were traced using Fiji software, as previously described.[41] Vessel length density (VLD) was calculated by using the following formula: total vessel length (mm)/area of quantification (mm^2). Several fields were randomly selected, covering

https://doi.org/10.1021/acsbiomaterials.4c01594
ACS Biomater. Sci. Eng. 2025, 11, 1583−1597

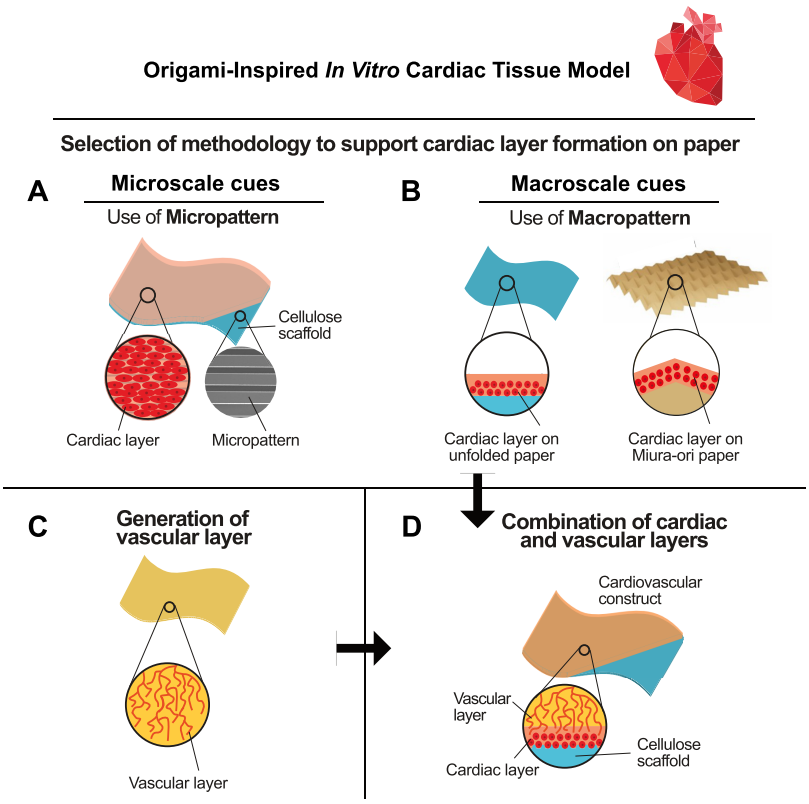

Figure 1. Schematic representation of the experimental design for the origami-inspired *in vitro* cardiac tissue model. The design employs micro- and macroscale-based strategies to cellulose scaffolds to support tissue formation: (A) development of micropatterns for cardiac layer organization, (B) application of the Miura-ori micropattern for structural support, (C) formation of a vascular layer, and (D) integration of the cardiac and vascular layers to form a cardiovascular construct on an unfolded cellulose scaffold.

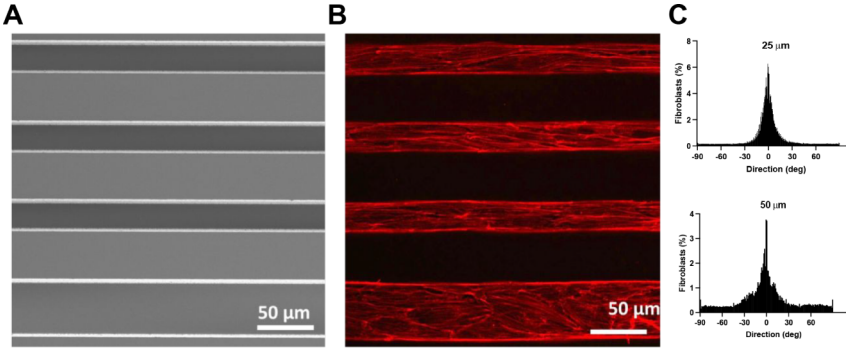

Figure 2. Cell alignment on different patterns. (A) Scanning electron microscopy images of PDMS molds and rat fibroblast (ATCC CRL-1764) alignment on patterned substrates. PDMS replica from custom-made SU8 microfabricated molds. (B) Rhodamine-phalloidin staining of rat2 fibroblasts grown on cross-linked 10% w/v gelatin hydrogels patterned with the PDMS molds showed good alignment on 25 and 50 μm wide structures (CLSM image of the bottom surface). (C) Directionality histograms of the actin cytoskeleton of cells growing on the 25 and 50 μm structures shown in panel (B). Scale bars: 50 μm.

at least 10% of the overall z-stack of each construct, and the individual results were averaged to yield a single value for each biological replicate. Furthermore, to ensure the absence of bias, all analyses were performed by a blinded operator.

2.11. Cardiac Functional Analysis. After 6 days of culture, cell contractile activity in response to electrical field stimulation was assessed by measuring two parameters of electrical maturation (excitation threshold (ET) and maximum capture rate (MCR)).[42] The pacing tests were performed inside a live-imaging microscope incubator (ZEISS X91, Olympus, Japan) with temperature (37 °C) and carbon dioxide (5%) control. For the 2D gelatin substrate, electrical pulses (2 ms duration, 1 Hz) were imposed using a custom-made electrical stimulator[40] with an increasing voltage amplitude starting from 1 V/cm to determine the minimal electrical field capable of generating a synchronous cell contraction (ET). For functional analysis of paper-based scaffolds, a different custom-made electrical stimulator[33] capable of reaching a higher voltage amplitude (30 V) was used. Once ET was established, the maximum imposed frequency that the cells can follow (MCR) was evaluated by varying the frequency of the pulses while maintaining the electrical field equal to 150% ET. For the functional analysis, a custom-made electrical stimulation chamber, with a distance of the carbon rod electrodes of 1 cm, was used.[40] Videos of the stimulated cells under electrical pacing were acquired using 4× and 10× objective lenses at 30 fps with a live-imaging microscope incubator.

https://doi.org/10.1021/acsbiomaterials.4c01594
ACS Biomater. Sci. Eng. 2025, 11, 1583−1597

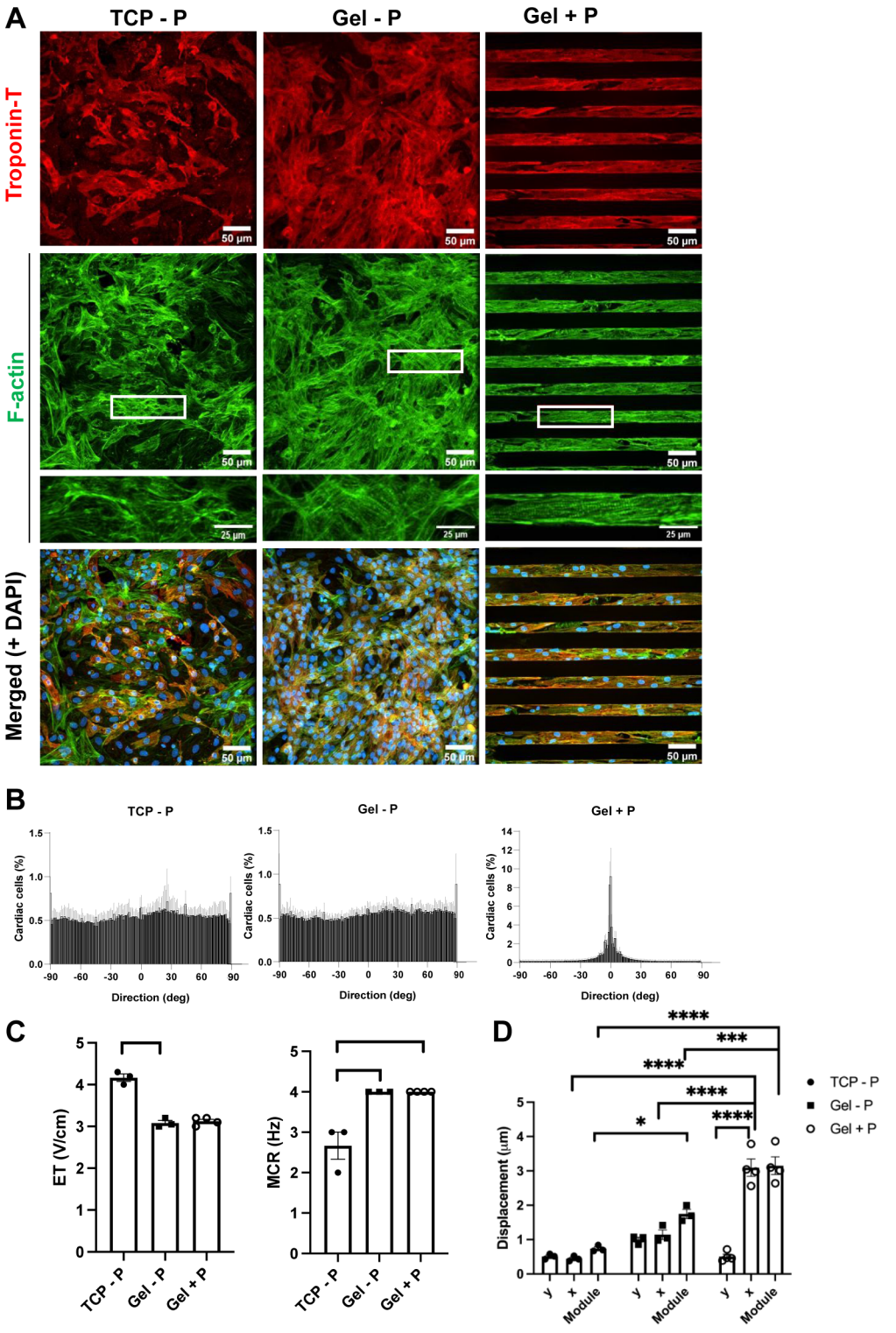

Figure 3. Effects of pattern on cardiac cell alignment and functionality. (A) Representative immunofluorescence images of cells cultured on the tissue culture plate (TCP − P), gelatin with a pattern (gel + P), or gelatin without a pattern (gel − P). The cells were stained for troponin-T (red) and F-actin (green), while the nuclei were stained with DAPI (blue). (B) Histograms depicting the directionality of cells in the three culture conditions. (C) Functional properties of the cells cultured on TCP − P ($n = 3$ replicates), gel − P ($n = 3$ replicates), and gel + P ($n = 4$ replicates) following exposure to external electrical pacing: excitation threshold (ET) and maximum capture rate (MCR). Statistical analysis was performed using Mann−Whitney's nonparametric test. (D) Displacement of NRCMs along the *y*-axis, *x*-axis, and its module for the three experimental groups. Statistical analysis was performed using a two-way ANOVA test. * denotes a statistically significant difference (*$p < 0.05$, **$p < 0.005$, ***$p < 0.0005$, ****$p < 0.0001$).

Since the matrix of the paper did not allow the contraction of individual cells to be observed, the displacement of its edges was analyzed instead to evaluate ET and MCR.

To evaluate the direction and modules of the displacements of cell beats, the videos acquired during the functional analysis were assessed with TrackMate, an ImageJ tracking plugin. The videos, in ImageJ, were

https://doi.org/10.1021/acsbiomaterials.4c01594
ACS Biomater. Sci. Eng. 2025, 11, 1583−1597

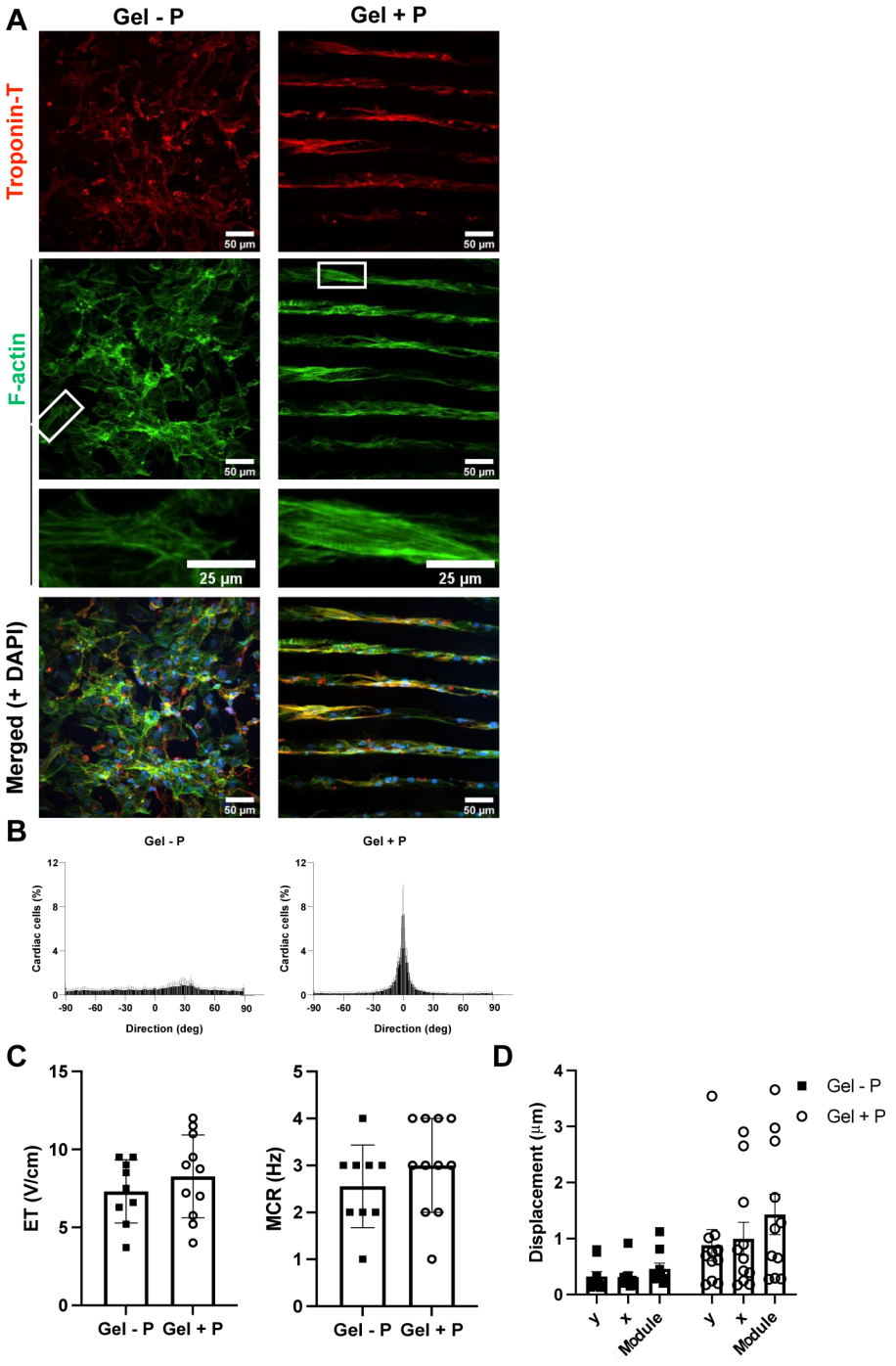

Figure 4. Effects of paper support with or without the micropatterned gelatin on cardiac cell alignment and functionality. (A) Representative immunofluorescence images of cells cultured on paper supports in the presence of gelatin with pattern (gel + P) or without pattern (gel − P). Cells were stained for troponin-T (red) and F-actin (green), while the nuclei were stained with DAPI (blue). (B) Histograms showing the directionality of the cells cultured on paper on gelatin without pattern, bottom of gelatin with pattern, and top of gelatin with pattern. (C) Functional properties of cells cultured on paper on gelatin with (n = 11 replicates) and without pattern (n = 9 replicates). Statistical analysis was performed using a nonparametric test. (D) Displacement of the paper along the y-axis, x-axis, and the module of displacement. Statistical analysis was performed using a two-way ANOVA test.

divided in frame, and each frame corresponds to 0.033 s of videos since the videos were acquired at 30 fps. In TrackMate, the threshold was set in order to have around 800 points, with a diameter of 10 μm, to track. The program tracked the movement of points through the different frames and generated their trajectory. The trajectories were eliminated if they had gap of tracking, their displacements were greater than 15 μm between 2 frames, or the tracking duration was shorter than the duration of the video. In this way, false trajectories were excluded.

Forty trajectories, out of the approximately 800 detected, were randomly selected for manual reanalysis to ensure that the trajectory corresponded exactly to the movement of the cells. The X and Y coordinates of the trajectories were exported to an Excel file, and the signals were processed with a custom MatLab code. In short, the X and Y coordinates were subtracted from the coordinates of the points of the temporal instant in which the cardiomyocytes were relaxed in order to

https://doi.org/10.1021/acsbiomaterials.4c01594
ACS Biomater. Sci. Eng. 2025, 11, 1583−1597

Table 1. Average and Standard Deviation of the Elastic Modulus Measured for all the Gelatin Samples at 37 °C

Gelatin (%)		Elastic modulus (kPa)			
		4	6	9	12
TG (mg/mL)	50	ND	2.07 ± 0.39	6.78 ± 0.85	12.10 ± 0.21
	100	1.70 ± 0.35	5.20 ± 0.14	15.71 ± 2.66	19.09 ± 1.02

obtain the values expressed in displacement along the *X* and *Y* axes. The magnitude of the displacement was also calculated.

2.12. Statistical Analysis. Image quantification was performed for cell alignment on at least 9 images for each sample. All data are presented as mean ± standard error of the mean (SEM), except for Figures 2C, 3B, 4B, 4C, 6C, and 6D, in which data are presented as means ± standard deviation (SD). One-way or two-way ANOVA test was used for normally distributed populations (Figures 3D and 4D). For all other graphs, nonparametric Mann−Whitney's test and Kruskal−Wallis's test were used for single and multiple comparisons, respectively. Statistical analyses were conducted using GraphPad Prism 9 (GraphPad Software, Inc., USA). Statistical significance was set at $p < 0.05$.

3. RESULTS

Building on the proposal to use a cellulose substrate for facilitating the formation and manipulation of cell constructs while supporting mechanical contraction, two strategies, microscale and macroscale approaches, were explored to enable cardiac layer contraction on paper (Figure 1A,B). Furthermore, a vascular layer was generated and incorporated to assess the *in vitro* feasibility of coculturing the two layers while preserving both cardiac contraction and vascularization potential (Figure 1C,D).

3.1. Micropatterning Strategy to Support Cardiac Cell Function on Paper Substrates. To explore the effects of micropatterned physical cues on cardiac cell alignment and functionality, a gelatin-based micropatterning strategy was developed (Figure 1A). The mechanical and functional properties of these substrates were evaluated to assess their potential to support cardiac contraction on cellulose scaffolds.

3.1.1. Gelatin-Based Micropattern Characterization. Based on the need for substrates that provide cell alignment, it was investigated how different gelatin patterns influence cellular orientation and mechanical properties, setting the stage for their application in cardiac cell culture. The alignment of cells in linear grooves is known to be influenced by the lateral dimensions and the surface roughness of the substrate.[5,9,43] PDMS stamps were fabricated to transfer alignment cues into the gelatin hydrogel by a molding process. Scanning electron microscopy inspection of the PDMS stamp revealed smooth planar surfaces and confirmed the desired lateral dimensions of 25 and 50 μm (Figure 2A). The initial cell alignment assays were performed using embryo rat fibroblasts to assess cell adhesion, pattern fidelity, and surface quality. When cultured on gelatin samples patterned with the PDMS molds, cells aligned in the direction of the linear features of 25 and 50 μm, as indicated by the orientation of the cellular actin filaments (Figure 2B). Notably, the alignment was more pronounced in the narrower 25 μm structures compared to that in the 50 μm structures (Figure 2C). Based on these results, the 25 μm features were selected for the subsequent experiments involving cardiomyocytes.

The mechanical properties of gelatin are crucial for its use in cardiac tissue engineering applications, where it is commonly used as a substrate for cell attachment. The mechanical properties of the gelatin samples were characterized by nanoindentation in order to assess the substrate stiffness depending on the ratio between gelatin concentration and cross-linker enzyme concentration. The nanoindentation tests performed on the different gelatin compositions (4, 6, 9, and 12% w/v) enzymatically gelled with two different enzyme concentrations (50 or 100 mg/mL) revealed an average elastic modulus of the samples ranging between 1.70 ± 0.35 and 19.09 ± 1.02 kPa (Table 1). In particular, it can be noted that higher concentrations of gelatin correspond to higher substrate stiffness, and the amount of cross-linker enzyme plays a role as well, indeed doubling its concentration and increasing the stiffness. Considering the elastic modulus range of a healthy heart, which is typically between 10 and 20 kPa,[15,17,19] gelatin compositions of 9% cross-linked with 100 mg/mL TG (15.71 ± 2.66 kPa), 12% cross-linked with 50 mg/mL TG (12.10 ± 0.21 kPa), and 12% cross-linked with 100 mg/mL TG (19.09 ± 1.02 kPa) appear to be suitable options, as they fall within this specified range.

The selection of the appropriate hydrogel composition was also guided by evaluation of the cell functionality on the different substrates. A low ET and a high MCR value are considered indicative of advanced cardiac functionality. Cardiac cells cultured on a stiffer substrate exhibited a lower ET to those cultured on a soft hydrogel composition, although the difference was not statistically significant (Supplementary Figure S1). Considering altogether mechanical properties and ET and MCR values, both the 9% w/v gelatin with TG 100 mg/mL and 12% w/v gelatin with TG 100 mg/mL compositions would be suitable for further use.[27] However, due to the superior reproducibility (low standard deviation) and a high MCR observed in the 12% w/v gelatin cross-linked with 100 mg/mL TG composition, the latter was chosen for subsequent experiments.

3.1.2. Cardiac Cell Alignment on Micropatterned Gelatin Substrates. After selecting the 25 μm dimension as the optimal size of the gelatin pattern for enhancing cellular alignment, the impact of micropatterns on the maturation and functionality of cardiac cells was studied compared to nonpatterned substrates. Culture on smooth gelatin substrates without a pattern served as controls. The immunofluorescence images clearly demonstrated that only cells cultured on patterned gelatin exhibited alignment along the direction of the grooves (Figure 3A). Both NRCMs, identified as cardiac troponin-T-positive cells, and NRFBs, characterized as troponin-T-negative and F-actin-positive cells, showed alignment in accordance with the pattern. In contrast, the two control groups, consisting of cells cultured on standard TCP and gelatin substrates without any pattern, displayed a random arrangement of cells without any preferred direction. The organization of troponin-T in NRCMs, with or without the pattern, is visibly evident (Figure 3A).

The analysis of cell directionality confirmed the observed alignment pattern. In particular, the regions of the patterned gelatin showed a clear alignment of NRCMs along the grooves (Figure 3B). On the contrary, NRCMs cultured on gelatin without a pattern and on TCP displayed a random orientation without any preferential direction.

https://doi.org/10.1021/acsbiomaterials.4c01594
ACS Biomater. Sci. Eng. 2025, 11, 1583−1597

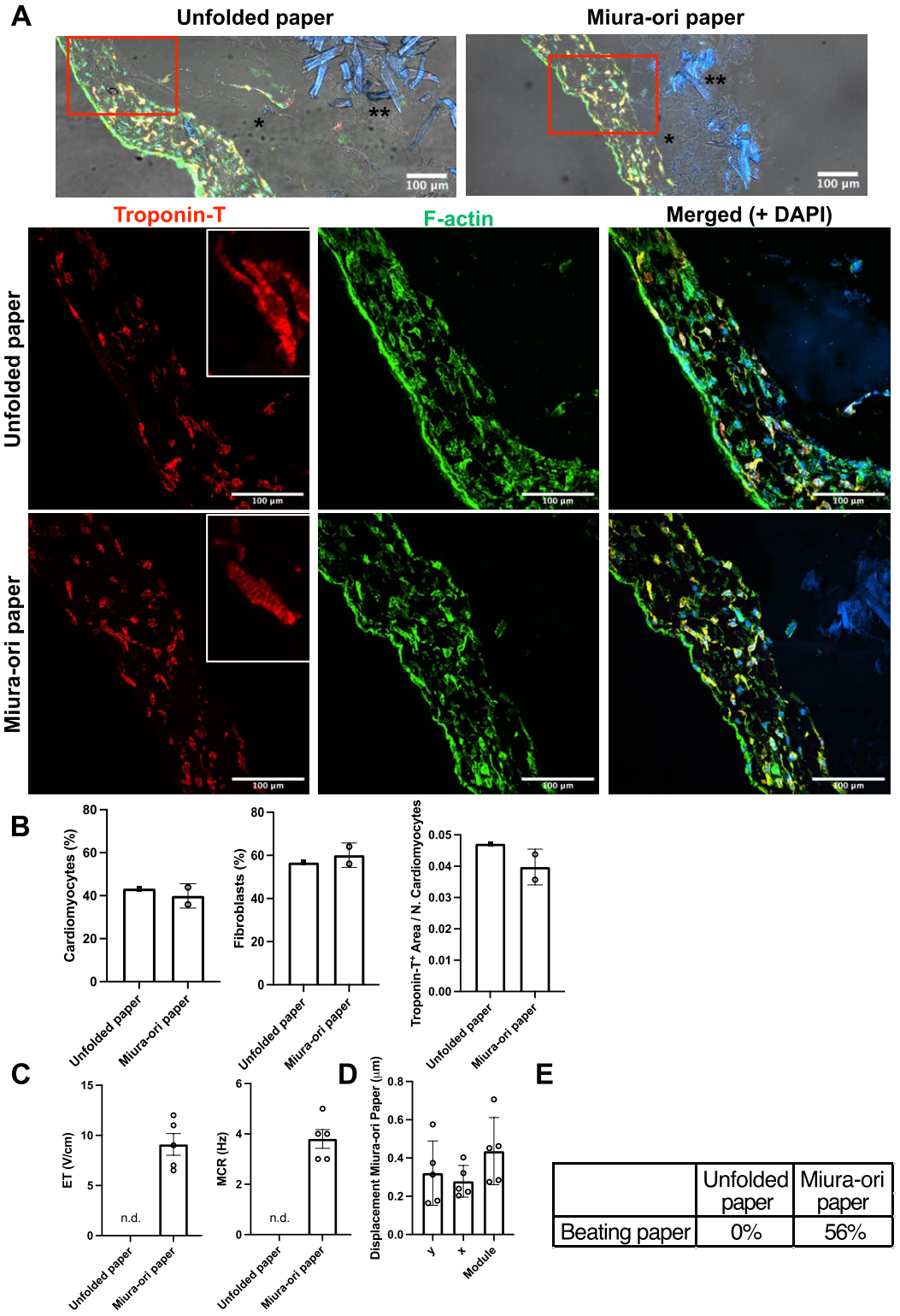

	Unfolded paper	Miura-ori paper
Beating paper	0%	56%

Figure 5. Effects of Miura-ori paper as a substrate for cardiac cell functionality. (A) Representative immunofluorescence images of cells cultured on unfolded and Miura-ori paper. Gelatin is indicated by *, while the paper's filaments are indicated by **. The cells were stained for troponin-T (red) and F-actin (green), and the nuclei were stained in DAPI (blue). (B) Image-based quantification of the percentage of cardiomyocytes and fibroblasts and the percentage of area positive for troponin-T normalized by the number of cardiomyocytes for the unfolded (n = 1 replicates) and Miura-ori paper (n = 2 replicates). (C) Functional properties of cells cultured on unfolded (n = 9 replicates) and Miura-ori paper (n = 9 replicates). (D) Displacement of the folded paper along the y-axis, x-axis, and the module of the displacement. (E) Percentage of beating cells for unfolded and Miura-ori papers.

Subsequent electrical stimulation of the samples allowed for the evaluation of two functional parameters, ET and MCR. Compared to cells cultured on TCP (ET = 4.17 ± 0.15 V/cm and MCR = 2.67 ± 0.58 Hz), the use of gelatin without pattern as a substrate led to a significant decrease in ET (3.13 ± 0.10 V/cm) and an increase in MCR (4 ± 0 Hz) of cardiac cells,

https://doi.org/10.1021/acsbiomaterials.4c01594
ACS Biomater. Sci. Eng. 2025, 11, 1583−1597

indicating the importance of having a substrate with a stiffness resembling muscle tissue to promote cardiac maturation and contractility (Figure 3C). However, the presence of a pattern on the gelatin substrate did not improve the functionality of NRCMs. In fact, the ET and MCR values were similar for NRCMs cultured on gelatin with and without a pattern (ET = 3.08 ± 0.10 V/cm and MCR = 4 ± 0 Hz).

Analyzing the displacement of NRCMs in the functional videos, the effect of the pattern's presence became evident. Cells cultured on gelatin with a pattern exhibited significantly higher displacement along the pattern's direction (x-axis) and a higher module of displacement (x = 2.95 ± 0.54 μm; module = 3.03 ± 0.52 μm) (Supplementary Video S1) compared to the cells cultured on gelatin without a pattern (x = 1.15 ± 0.23 μm; module = 1.75 ± 0.23 μm) (Supplementary Video S2) and on TCP (x = 0.44 ± 0.08 μm; module = 0.74 ± 0.09 μm) (Supplementary Video S3) (Figure 3D). Furthermore, in the presence of the pattern on gelatin, the prevailing direction of contraction was along the x-axis, indicating that the pattern significantly influenced the direction of contraction. Interestingly, NRCMs cultured on a substrate mimicking the stiffness of soft tissues exhibited a higher module of displacement compared with NRCMs on TCP (Figure 3D).

3.1.3. Cardiac Cell Functionality on Micropatterned Gelatin-Based Paper Substrates. Building on the previous results from gelatin substrates prompted the integration of gelatin-based micropatterns onto the paper scaffolds. Micropatterning has previously been shown to enhance the functionality and alignment of cardiac cells in a 2D culture. We investigated the impact of micropatterning on the movement of paper substrates during cell contraction. Immunofluorescence imaging confirmed that cardiac cells cultured on smooth gelatin substrates layered on top of the paper exhibited a random organization. On the contrary, cardiac cells cultured on patterned gelatin showed well-aligned cells in the direction of the groove (Figure 4A).

The results of the image analysis confirmed that cells aligned only in the presence of a pattern. The histogram displayed a normal distribution, which was centered on the direction of the grooves, while a random distribution of peaks was observed on the smooth gelatin-covered paper (Figure 4B). However, based on the functional test, the presence of the pattern on gelatin and the subsequent cell alignment did not improve paper functionality. The ET and MCR were similar for cells cultured on papers with (8.04 ± 2.70 and 2.89 ± 1.05 Hz, respectively) and without patterns (7.31 ± 2.03 and 2.56 ± 0.88 Hz, respectively) (Figure 4C).

By analyzing the displacement of the paper in the functional videos, we observed an effect of the presence of the pattern. The paper with the pattern displayed a trend of increase in the displacement (module = 1.43 ± 1.20 μm) (Supplementary Video S4) compared to the paper without the pattern (module = 0.46 ± 0.31 μm) (Supplementary Video S5), although the difference was not statistically significant. Interestingly, in this particular experimental setup, the presence of the pattern did not have an impact on the direction of contraction (Figure 4D).

3.2. Origami-Inspired Macro-Pattern Strategy to Support Cardiac Cell Function on Paper Substrates. Given the lack of significant functional improvements observed with micropatterned substrates layered on paper scaffolds, a Miura-ori-inspired macropatterning approach was introduced (Figure 1B). This strategy leverages the mechanical movement of paper scaffolds to enhance the contractility of cardiac constructs. To evaluate the potential benefits of paper movement on cell contraction, the Miura-ori origami technique was applied to create a macropatterned surface on the paper. Cardiac cells were then embedded in fibrin gels, providing a more biomimetic environment and increasing the number of cells contributing to the construct's movement. The cells were cultured on both Miura-ori papers (with the micropattern) and unfolded papers (as control). Brightfield images revealed the presence of paper filaments (indicated with ** in images) and gelatin (indicated with *) (Figure 5A). The organization of cardiac troponin-T in the NRCMs appeared similar in both Miura-ori and unfolded paper conditions, with a mature-like cell sarcomeric organization observed (Figure 5A). In particular, additional analyses comparing the composition and maturation of cardiomyocytes and fibroblasts between the folded and unfolded paper conditions revealed comparable numbers of these two cell types under both conditions. Specifically, the folded paper cultures consisted of 39.9 ± 5.7% NRCMs and 60.0 ± 5.6% NRFBs, while the unfolded paper cultures had 43.3% NRCMs and 56.7% NRFBs (Figure 5B). Moreover, the quantification of the troponin-T positive area normalized by the number of cardiomyocytes found no significant differences between the two groups (Figure 5B), further indicating that the absence of beating in the unfolded paper cultures was not due to variations in cell composition or NRCM maturation.

The functional evaluation (Figure 5C,E) demonstrated that the presence of the folds was essential for enabling paper contraction as none of the unfolded paper contracted. In contrast, a majority (56%) of the Miura-ori papers successfully contracted in response to external pacing (Supplementary Video S6). The module of displacement for the contracting Miura-ori paper was measured to be 0.44 ± 0.18 μm without a prevalent direction of contraction (Figure 5D).

3.3. Physiologically Differentiated Vascular Layer as a Strategy for Vascularization. Recognizing the importance of vascularization for supporting cell survival and functionality, a vascular layer was generated (Figure 1C), followed by the coculture of cardiac and vascular layers (Figure 1D). This study explores conditions that enable the formation of physiological microvascular networks (Figure 1C) while preserving the cardiac functionality. To develop contractile cardiac engineered tissues capable of promoting in vivo vascularization and supporting cell survival and function, we propose a multilayered approach for further studies. This approach involves integrating vascular layers with cardiac tissues generated using either gelatin-based micropatterned or Miura-ori-inspired paper techniques prior to implantation. One challenge in this process is the complexity of integrating the two layers, which first requires identifying conditions that allow for the physiological development and maturation of both cardiac and vascular tissues together. Therefore, NRCCs were cultured under vascular conditions (in EGM-2 medium) and compared to standard cardiac conditions (low-glucose DMEM). After 3 days of culture, NRCCs cultured with EGM-2 medium led to spontaneous beating (Supplementary Video S11) with contraction behavior similar to the NRCCs cultured with LG-DMEM supplemented with 1% v/v FBS, 1% v/v PS, 1% v/v HEPES, and 1% v/v L-Glu (Supplementary Video S12). To assess the level of cardiac maturation, the presence of specific cardiac proteins was investigated, namely, the gap-junction protein Cx-43 and the contractile sarcomeric α-actinin. Most of the cells cultured with EGM-2 medium and LG-DMEM were positive for Cx-43 (Supplementary Figure S2). In particular,

https://doi.org/10.1021/acsbiomaterials.4c01594
ACS Biomater. Sci. Eng. 2025, 11, 1583−1597

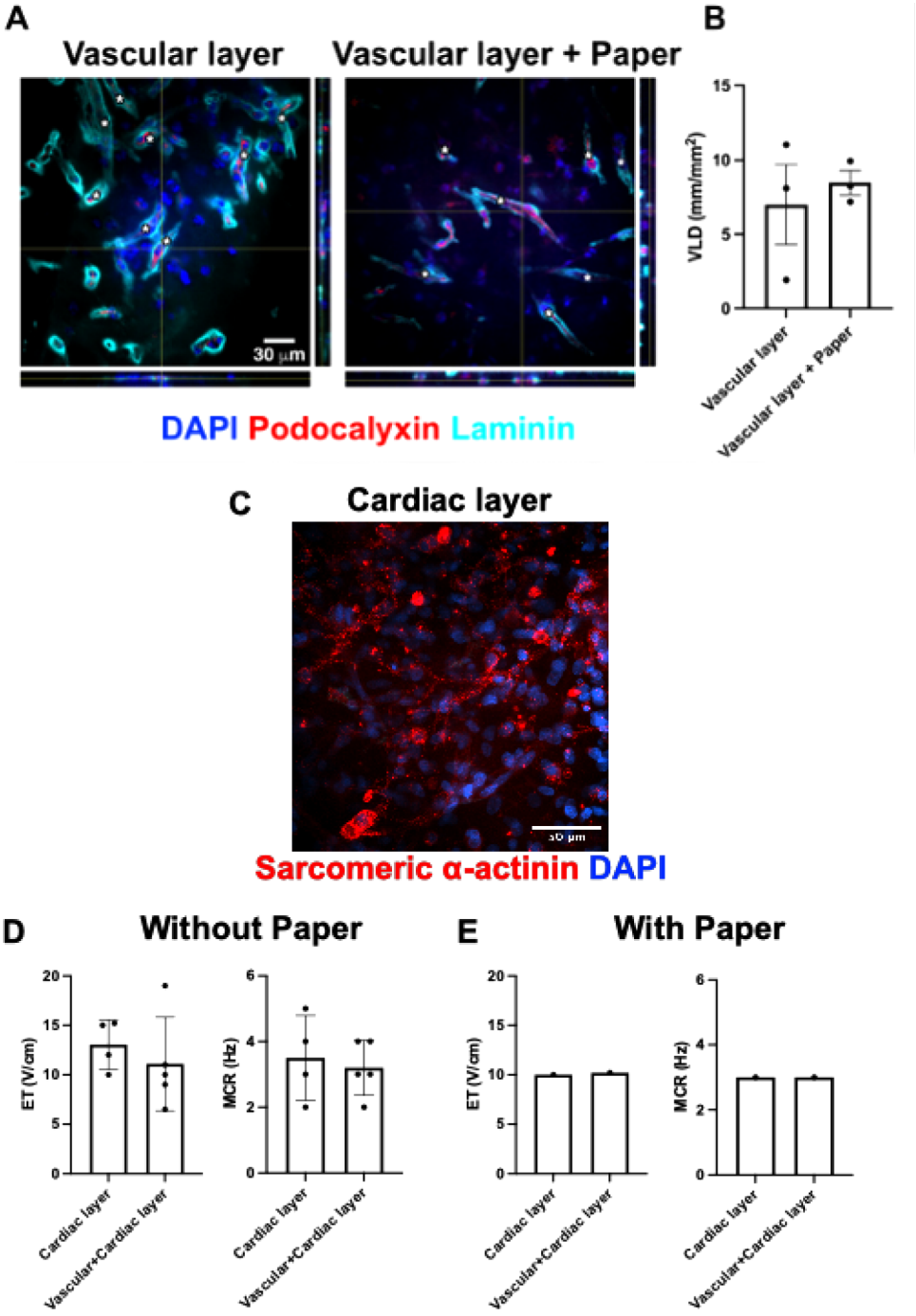

Figure 6. Immunostaining and functional test of 3D coculture of the vessel and cardiac layer. (A) Representative immunofluorescence images of polarized vessel formation in the absence and presence of paper as support. Cells were stained for podocalyxin (red) and laminin (cyan), and the nuclei were stained with DAPI (blue). The bottom and lateral pods display a vertical optical reconstruction through the z-stack along the indicated lines. Asterisks indicate vessels' lumens. (B) Quantification of the vascular structure in the absence and presence of paper as support (n = 3). Vessel length density (VLD). Statistical analysis was performed using a nonparametric test. (C) Representative immunofluorescence staining for sarcomeric α-actinin (red) of the cardiac layer in the coculture experiments. Cell nuclei were stained with DAPI (blue). (D) Electrical functionality of the cardiac layer (no. of replicates = 4) and the combination of vascular and cardiac layer (no. of replicates = 5) without the support of paper. Statistical analysis was performed using a nonparametric test. (E) Electrical functionality of the cardiac layer and the combination of vascular and cardiac layers with the support of paper (total number of replicates = 4, number of beating constructs = 1).

cells cultured with the EGM-2 medium were characterized by a higher expression of Cx-43 located in the cytoplasm and cell membrane in the proximity of neighboring NRCMs, suggesting its functional role as a gap junction. Similar sarcomere organization was observed with the two different culture media (Supplementary Figure S2). Based on these results, the vascular medium EGM-2 was selected for the coculture of cardiac and vascular layers.

Unfolded gelatin-stabilized paper was employed as a scaffold to support the cardiac layer, composed of a fibrin hydrogel. A second fibrin hydrogel layer containing vascular cells was overlaid on top of the cardiac layer. Physiological microvascular

https://doi.org/10.1021/acsbiomaterials.4c01594
ACS Biomater. Sci. Eng. 2025, 11, 1583−1597

networks rapidly self-assembled within 7 days of culture in both the presence and absence of paper (Figure 6A). Notably, the microvascular structures spontaneously formed patent lumens (asterisks in Figure 6A) and the endothelium displayed physiological apicobasal polarization, with podocalyxin expression restricted to the lumen-facing apical compartment and laminin deposition marking the basal side. Because self-assembled vascular structures are arranged in random directions, some are seen as circumferential shapes and others as longitudinal segments in the optical sections. The concentric sequence of basal laminin, apical podocalyxin, and central lumen can be appreciated also in the z-reconstructions shown in the lateral and bottom pods of panels in Figure 6A. The efficiency of microvascular network assembly was similar in both conditions, as shown by vessel length density quantification (Figure 6B), confirming that the combination with the cardiac layer did not interfere with the efficacy of the vascular layer formation. These data indicate that the formed vascular structures were physiologically differentiated and were not negatively affected by the presence of the cardiac layer (Figure 6C).

In the cardiac layer, the cardiomyocytes were partially elongated and displayed scattered organized sarcomeres (Figure 6C). Functional analysis without the paper showed beating of the construct when the cardiac layers alone or combined with the vascular layer were cultured with EGM-2 + 10% FBS (Figure 6D, Supplementary Videos S7 and S8).

A proof of concept for functionality was demonstrated using the paper as a scaffold; namely, constructs exhibited beating when the cardiac layer was cultured alone or combined with the vascular layer, but this effect was observed in only one out of four constructs. Notably, the presence of the paper as a supportive structure led to a reduction in beating (Figure 6E and Supplementary Videos S9 and S10).

4. DISCUSSION AND CONCLUSION

Here, we present a novel method for developing aligned and contractile ECTs, combined with a layer of physiologically differentiated microvascular networks, using Miura-ori gelatin-stabilized paper and fibrin hydrogels. The use of easily accessible hydrogel materials and cellulose paper makes this method cost-effective and scalable compared with conventional scaffolds such as Matrigel. In addition, the cellulose scaffold offers superior handling capabilities and scalability while maintaining in-plane contractibility, making it suitable for future applications as a cardiac patch in surgical interventions.

Existing studies in the literature[15,17,19] have consistently demonstrated that providing a substrate with stiffness similar to that of native cardiac tissue enhances the maturation and electrical properties of the NRCMs. In our study, while the use of a micropattern to align the cardiac cells did not significantly enhance their functional properties, it played a crucial role in achieving stronger and more highly directional cell contraction, which is essential for engineered cardiac tissues. This finding is in agreement with previous research and highlights the importance of structural cues in promoting appropriate tissue function.[5,9]

Initially, it was assumed that culturing NRCMs on gelatin would facilitate the formation of functional cell−cell connections necessary for synchronous tissue contraction. Additionally, it was supposed that directional cell orientation would contribute to intercellular functional communication and promote contraction directionality.

However, interestingly, NRCMs cultured on patterned gelatin-coated flat paper scaffolds showed only a slight increase in contraction amplitude (1.43 ± 1.20 μm vs 0.46 ± 0.31 μm) compared to cultures without an alignment pattern or contraction directionality. This suggests that the in-plane stiffness of the unfolded paper scaffolds may be too high relative to the NRCM contraction force, thereby hindering movement in alignment with the micropattern. The tensile strength (4.7 MPa) and elastic modulus (0.8 ± 0.1 GPA) of the paper scaffold were significantly higher than physiological values. Native cardiac tissue typically exhibits a Young's modulus of approximately 10−20 kPa,[15,17,19] which corresponds to a much lower tensile strength. This disparity may have contributed to the increased stiffness of the material, potentially limiting the effectiveness of the micropatterns. On the other hand, NRCMs grown on Miura-ori papers exhibited significant scaffold contraction (0.44 ± 0.18 μm vs none) compared to tissue grown on unfolded paper, demonstrating the importance of a Miura-ori macro-pattern in enabling lateral contractibility of the cellulose scaffold. The effect is particularly evident considering the similar maturation state of myocardial tissue on unfolded and Miura-ori scaffolds.

It is worth noting that the ET of cells cultured on papers with a pattern was superior (8.04 ± 2.70 versus 3.13 ± 0.10 V/cm), and the MCR was lower (2.89 ± 1.05 versus 4 ± 0 Hz) compared to cells cultured without paper support, confirming that paper is an obstacle for the contraction.

On the other hand, cells cultured on papers with pattern showed similar functional results compared to cells cultured on Miura-ori paper, with similar ET (8.04 ± 2.70 versus 9.10 ± 2.41 V/cm) and MCR (2.89 ± 1.05 versus 3.8 ± 0.84 Hz, respectively). Nevertheless, under both conditions, cardiac cells demonstrated the ability to pull the paper during their contractions.

Despite using the same paper composition, the cardiac cells cultured on Miura-ori paper exhibited superior contraction amplitude compared to those on a planar paper scaffold. This enhancement of beating observed in the Miura-ori paper compared to flat paper might be due to the macropattern since no major differences were noticed in the cardiac cell maturation or in the percentage of cardiomyocytes to justify the observed better contraction. However, further investigation of the mechanical properties arising from different Miura-ori pattern geometries and paper compositions would be beneficial to further support these first promising results. Moreover, the here-presented findings suggest that the force generated by a single layer of NRCMs may not always be sufficient to counteract the intrinsic stiffness of the paper although the paper grammage was selected in order to achieve mechanical properties favorable for cardiac tissue maturation during cell culture conditions.[31] To further address this challenge, thicker cell layers with higher cell densities are required. One possible approach is to stack and culture multiple layers of hydrogel and cells, which could help with the limitation of a single layer. However, maintaining viability becomes a crucial limitation for thicker tissues, necessitating vascularization. Therefore, here, we showed that a vascular layer can be cocultured with the ECT, forming physiologically differentiated and lumenized microvascular structures within a similar time frame as the NRCM maturation. Interestingly, when the cardiac layer was combined with the vascular layer, without the use of paper as a culture support, the constructs exhibited contractile behavior. However, when these constructs were cultured on unfolded gelatin-

https://doi.org/10.1021/acsbiomaterials.4c01594
ACS Biomater. Sci. Eng. 2025, 11, 1583−1597

stabilized papers, their contraction and movement were impaired or reduced. This observation aligns with the previous findings when culturing NRCMs alone on unfolded gelatin-stabilized papers, suggesting that the in-plane stiffness of flat paper scaffolds might be too high in relation to NRCM contraction. Furthermore, this emphasizes the potential advantages of using Miura-ori cellulose scaffolds to enhance the contraction.

Alternatively, 3D bioprinting may offer a more direct method for achieving nutrient diffusion into tissue. Recently, a bioink made of gelatin was developed,[27] which could be used to extrude multiple layers of cell-laden hydrogel onto Miura-ori paper. In addition, bioprinted cardiomyocyte patterns in multiple layers on Miura-ori paper could promote cell alignment and directional tissue contraction, similar to micropatterns. This combination of micro- and macropatterns has the potential to enhance the paper's ability to support and follow cell contraction.

Taken together, this work clearly demonstrated that hydrogel micropatterns and Miura-ori paper can promote both cell alignment and directional contraction. The Miura-ori folding, in particular, proved to be essential to enable functional contraction of an engineered cardiac monolayer.

■ ASSOCIATED CONTENT

Supporting Information

The Supporting Information is available free of charge at https://pubs.acs.org/doi/10.1021/acsbiomaterials.4c01594.

Additional experimental details; materials and methods; results including graphs of cardiac functionality on gelatin substrates with different stiffness (Figure S1); images and graphs on the effects of different culture media on cardiac cell maturation (Figure S2) (PDF)

Contraction of cardiomyocytes cultured on gelatin with pattern (Video S1) (MP4)

Contraction of cardiomyocytes cultured on gelatin without pattern (Video S2) (MP4)

Contraction of cardiomyocytes cultured on tissue culture plate (Video S3) (MP4)

Movement of patterned gelatin-based paper substrate used as cell support for cardiac cells (Video S4) (MP4)

Movement of smooth gelatin-based paper substrate used as cell support for cardiac cells (Video S5) (MP4)

Movement of the origami-folded paper used as cell support for cardiac cells (Video S6) (MP4)

Contraction of the cardiac layer alone without the paper support (Video S7) (MP4)

Contraction of the cardiac layer combined with the vascular layer without the paper support (Video S8) (MP4)

Contraction of the cardiac layer alone with the paper support (Video S9) (MP4)

Contraction of the cardiac layer combined with the vascular layer with the paper support (Video S10) (MP4)

Spontaneous beating of cardiomyocytes cultured with EGM-2 medium (Video S11) (MP4)

Spontaneous beating of cardiomyocytes cultured with LG DMEM supplemented with 1% v/v FBS, 1% v/v PS, 1% v/v HEPES, and 1% v/v L-Glu (Video S12) (MP4)

■ AUTHOR INFORMATION

Corresponding Author

Anna Marsano − *Department of Surgery, University Hospital Basel, Basel 4031, Switzerland; Department of Biomedicine, University Hospital Basel and University of Basel, Basel 4031, Switzerland;* orcid.org/0000-0002-3084-0823; Email: anna.marsano@usb.ch

Authors

Antonio Sileo − *Department of Surgery, University Hospital Basel, Basel 4031, Switzerland; Department of Biomedicine, University Hospital Basel and University of Basel, Basel 4031, Switzerland*

Federica Montrone − *Department of Surgery, University Hospital Basel, Basel 4031, Switzerland; Department of Biomedicine, University Hospital Basel and University of Basel, Basel 4031, Switzerland*

Adelin Rouchon − *Department of Surgery, University Hospital Basel, Basel 4031, Switzerland; Department of Biomedicine, University Hospital Basel and University of Basel, Basel 4031, Switzerland*

Donata Trueb − *Institute for Medical Engineering and Medical Informatics, University of Applied Sciences and Arts Northwestern Switzerland, Muttenz 4132, Switzerland*

Jasmin Selvi − *Institute for Medical Engineering and Medical Informatics, University of Applied Sciences and Arts Northwestern Switzerland, Muttenz 4132, Switzerland*

Moritz Schmid − *Institute for Medical Engineering and Medical Informatics, University of Applied Sciences and Arts Northwestern Switzerland, Muttenz 4132, Switzerland*

Julian Graef − *Institute for Chemistry and Bioanalytics, University of Applied Sciences and Arts Northwestern Switzerland, Muttenz 4132, Switzerland*

Fabian Züger − *Institute for Medical Engineering and Medical Informatics, University of Applied Sciences and Arts Northwestern Switzerland, Muttenz 4132, Switzerland*

Gianpaolo Serino − *Department of Mechanical and Aerospace Engineering and PolitoBIOMed Lab, Politecnico di Torino, Turin 10129, Italy*

Diana Massai − *Department of Mechanical and Aerospace Engineering and PolitoBIOMed Lab, Politecnico di Torino, Turin 10129, Italy*

Nunzia Di Maggio − *Department of Surgery, University Hospital Basel, Basel 4031, Switzerland; Department of Biomedicine, University Hospital Basel and University of Basel, Basel 4031, Switzerland*

Gabriela Melo Rodriguez − *Omya International AG, Egerkingen 4622, Switzerland*

Joachim Köser − *Institute for Chemistry and Bioanalytics, University of Applied Sciences and Arts Northwestern Switzerland, Muttenz 4132, Switzerland*

Joachim Schoelkopf − *Omya International AG, Egerkingen 4622, Switzerland*

Andrea Banfi − *Department of Surgery, University Hospital Basel, Basel 4031, Switzerland; Department of Biomedicine, University Hospital Basel and University of Basel, Basel 4031, Switzerland*

Maurizio Gullo − *Institute for Medical Engineering and Medical Informatics, University of Applied Sciences and Arts Northwestern Switzerland, Muttenz 4132, Switzerland*

Complete contact information is available at: https://pubs.acs.org/10.1021/acsbiomaterials.4c01594

Author Contributions

[▽]A.M. and M.G. have contributed equally to this work. A.M., M.G., and J.S. conceived the study. A.S., F.M., J.K., N.D.M., A.B., and A.M. designed the biological experiments. G.M., M.G., F.Z., and J.S. produced the paper. A.S., D.T., Ja.S., F.Z., M.S., J.G., and M.G. produced the gelatin. F.M., G.S., and D.M. characterized the gelatin. J.K. and J.G. produced and tested the PDMS pattern. A.S., F.M., A.R., and J.K. performed the biological experiment and assessments. A.S., J.K., A.R., and F.M. analyzed the biological data. A.S., A.R., N.D.M., and J.K. prepared the figures. N.A.S., A.M., and M.G. reviewed the state of art. A.S., A.M., J.K., A.B., and M.G. wrote the manuscript.

Notes

The authors declare no competing financial interest.

■ ACKNOWLEDGMENTS

The authors thank Stefano Gabetti for the use of the custom-made electrical stimulator (ELETTRA) for the cardiac functional analysis on 2D gelatin substrate. The financial support from the Swiss Nanoscience Institute (SNI) Nano Argovia Project KOKORO (A14.07) is gratefully acknowledged. The project was also supported by the SNSF grant (310030_172989).

■ REFERENCES

(1) Huethorst, E.; Mortensen, P.; Simitev, R. D.; Gao, H.; Pohjolainen, L.; Talman, V.; Ruskoaho, H.; Burton, F. L.; Gadegaard, N.; Smith, G. L. Conventional Rigid 2D Substrates Cause Complex Contractile Signals in Monolayers of Human Induced Pluripotent Stem Cell-Derived Cardiomyocytes. *J. Physiol.* **2022**, *600* (3), 483−507.

(2) Jabbour, R. J.; Owen, T. J.; Pandey, P.; Reinsch, M.; Wang, B.; King, O.; Couch, L. S.; Pantou, D.; Pitcher, D. S.; Chowdhury, R. A.; et al. In Vivo Grafting of Large Engineered Heart Tissue Patches for Cardiac Repair. *JCI Insight* **2021**, *6* (15), 144068.

(3) Querdel, E.; Reinsch, M.; Castro, L.; Köse, D.; Bähr, A.; Reich, S.; Geertz, B.; Ulmer, B.; Schulze, M.; Lemoine, M. D.; et al. Human Engineered Heart Tissue Patches Remuscularize the Injured Heart in a Dose-Dependent Manner. *Circulation* **2021**, *143* (20), 1991−2006.

(4) Hosseinzadeh, E.; Sigaroodi, F.; Ganjoury, C.; Parandakh, A.; Najmoddin, N.; Shahriari, S.; Maymand, M. M.; Khani, M.-M. Cardiomyocyte Differentiation of Umbilical Cord Mesenchymal Stem Cells on Poly(Mannitol Sebacate)/Multi-Walled Carbon Nanotube Substrate. *Polym. Int.* **2024**, *73* (10), 844−851.

(5) Zhang, F.; Zhang, N.; Meng, H.-X.; Liu, H.-X.; Lu, Y.-Q.; Liu, C.-M.; Zhang, Z.-M.; Qu, K.-Y.; Huang, N.-P. Easy Applied Gelatin-Based Hydrogel System for Long-Term Functional Cardiomyocyte Culture and Myocardium Formation. *ACS Biomater. Sci. Eng.* **2019**, *5* (6), 3022−3031.

(6) Annabi, N.; Tsang, K.; Mithieux, S. M.; Nikkhah, M.; Ameri, A.; Khademhosseini, A.; Weiss, A. S. Highly Elastic Micropatterned Hydrogel for Engineering Functional Cardiac Tissue. *Adv. Funct. Mater.* **2013**, *23* (39), 4950−4959.

(7) Au, H. T. H.; Cui, B.; Chu, Z. E.; Veres, T.; Radisic, M. Cell Culture Chips for Simultaneous Application of Topographical and Electrical Cues Enhance Phenotype of Cardiomyocytes. *Lab Chip* **2009**, *9* (4), 564−575.

(8) Parrag, I. C.; Zandstra, P. W.; Woodhouse, K. A. Fiber Alignment and Coculture with Fibroblasts Improves the Differentiated Phenotype of Murine Embryonic Stem Cell-Derived Cardiomyocytes for Cardiac Tissue Engineering. *Biotechnol. Bioeng.* **2012**, *109* (3), 813−822.

(9) Napiwocki, B. N.; Lang, D.; Stempien, A.; Zhang, J.; Vaidyanathan, R.; Makielski, J. C.; Eckhardt, L. L.; Glukhov, A. V.; Kamp, T. J.; Crone, W. C. Aligned Human Cardiac Syncytium for in Vitro Analysis of Electrical, Structural, and Mechanical Readouts. *Biotechnol. Bioeng.* **2021**, *118* (1), 442−452.

(10) Rosellini, E.; Cascone, M. G.; Guidi, L.; Schubert, D. W.; Roether, J. A.; Boccaccini, A. R. Mending a Broken Heart by Biomimetic 3D Printed Natural Biomaterial-Based Cardiac Patches: A Review. *Front. Bioeng. Biotechnol.* **2023**, *11*, 1254739.

(11) Nikolova, M. P.; Chavali, M. S. Recent Advances in Biomaterials for 3D Scaffolds: A Review. *Bioact. Mater.* **2019**, *4*, 271−292.

(12) Wu, J.; Guo, X.; Pan, X.; Hua, J.; Cen, Y.; Li, S.; Huang, F.; Zhang, F.; Pan, L.; Shi, Y. Origami-Kirigami Structures and Its Applications in Biomedical Devices. *Biomed. Mater. Devices* **2024**, 1−17.

(13) Akbarzadeh, A.; Sobhani, S.; Soltani Khaboushan, A.; Kajbafzadeh, A.-M. Whole-Heart Tissue Engineering and Cardiac Patches: Challenges and Promises. *Bioengineering* **2023**, *10* (1), 106.

(14) Bhullar, S. K.; Thingnam, R.; Kirshenbaum, E.; Nematisouldaragh, D.; Crandall, M.; Willerth, S. M.; Ramkrishna, S.; Rabinovich-Nikitin, I.; Kirshenbaum, L. A. Living Nanofiber-Enabled Cardiac Patches for Myocardial Injury. *JACC Basic Transl. Sci.*, **2024**, .

(15) Rodriguez, M. L.; Beussman, K. M.; Chun, K. S.; Walzer, M. S.; Yang, X.; Murry, C. E.; Sniadecki, N. J. Substrate Stiffness, Cell Anisotropy, and Cell−Cell Contact Contribute to Enhanced Structural and Calcium Handling Properties of Human Embryonic Stem Cell-Derived Cardiomyocytes. *ACS Biomater. Sci. Eng.* **2019**, *5* (8), 3876−3888.

(16) Berry, M. F.; Engler, A. J.; Woo, Y. J.; Pirolli, T. J.; Bish, L. T.; Jayasankar, V.; Morine, K. J.; Gardner, T. J.; Discher, D. E.; Sweeney, H. L. Mesenchymal Stem Cell Injection after Myocardial Infarction Improves Myocardial Compliance. *Am. J. Physiol.-Heart Circ. Physiol.* **2006**, *290* (6), H2196−H2203.

(17) Engler, A. J.; Carag-Krieger, C.; Johnson, C. P.; Raab, M.; Tang, H.-Y.; Speicher, D. W.; Sanger, J. W.; Sanger, J. M.; Discher, D. E. Embryonic Cardiomyocytes Beat Best on a Matrix with Heart-like Elasticity: Scar-like Rigidity Inhibits Beating. *J. Cell Sci.* **2008**, *121* (22), 3794−3802.

(18) Putten, S. V.; Shafieyan, Y.; Hinz, B. Mechanical Control of Cardiac Myofibroblasts. *J. Mol. Cell. Cardiol.* **2016**, *93*, 133−142.

(19) Heras-Bautista, C. O.; Mikhael, N.; Lam, J.; Shinde, V.; Katsen-Globa, A.; Dieluweit, S.; Molcanyi, M.; Uvarov, V.; Jütten, P.; Sahito, R. G. A.; Mederos-Henry, F.; Piechot, A.; Brockmeier, K.; Hescheler, J.; Sachinidis, A.; Pfannkuche, K. Cardiomyocytes Facing Fibrotic Conditions Re-Express Extracellular Matrix Transcripts. *Acta Biomater.* **2019**, *89*, 180−192.

(20) Münch, J.; Abdelilah-Seyfried, S. Sensing and Responding of Cardiomyocytes to Changes of Tissue Stiffness in the Diseased Heart. *Front. Cell Dev. Biol.* **2021**, *9*, 642840.

(21) Ng, K.; Gao, B.; Yong, K. W.; Li, Y.; Shi, M.; Zhao, X.; Li, Z.; Zhang, X.; Pingguan-Murphy, B.; Yang, H.; Xu, F. Paper-Based Cell Culture Platform and Its Emerging Biomedical Applications. *Mater. Today* **2017**, *20* (1), 32−44.

(22) Lantigua, D.; Kelly, Y. N.; Unal, B.; Camci-Unal, G. Engineered Paper-Based Cell Culture Platforms. *Adv. Healthcare Mater.* **2017**, *6* (22), 1700619.

(23) Qi, A.; Hoo, S. P.; Friend, J.; Yeo, L.; Yue, Z.; Chan, P. P. Y. Hydroxypropyl Cellulose Methacrylate as a Photo-Patternable and Biodegradable Hybrid Paper Substrate for Cell Culture and Other Bioapplications. *Adv. Healthcare Mater.* **2014**, *3* (4), 543−554.

(24) Wang, L.; Xu, C.; Zhu, Y.; Yu, Y.; Sun, N.; Zhang, X.; Feng, K.; Qin, J. Human Induced Pluripotent Stem Cell-Derived Beating Cardiac Tissues on Paper. *Lab Chip* **2015**, *15* (22), 4283−4290.

(25) Mosadegh, B.; Dabiri, B. E.; Lockett, M. R.; Derda, R.; Campbell, P.; Parker, K. K.; Whitesides, G. M. Three-Dimensional Paper-Based Model for Cardiac Ischemia. *Adv. Healthcare Mater.* **2014**, *3* (7), 1036−1043.

(26) Sapp, M. C.; Fares, H. J.; Estrada, A. C.; Grande-Allen, K. J. Multilayer Three-Dimensional Filter Paper Constructs for the Culture and Analysis of Aortic Valvular Interstitial Cells. *Acta Biomater.* **2015**, *13*, 199−206.

(27) Züger, F.; Berner, N.; Gullo, M. R. Towards a Novel Cost-Effective and Versatile Bioink for 3D-Bioprinting in Tissue Engineering. *Biomimetics* **2023**, *8* (1), 27.

https://doi.org/10.1021/acsbiomaterials.4c01594
ACS Biomater. Sci. Eng. 2025, 11, 1583−1597

(28) Yung, C. W.; Wu, L. Q.; Tullman, J. A.; Payne, G. F.; Bentley, W. E.; Barbari, T. A. Transglutaminase Crosslinked Gelatin as a Tissue Engineering Scaffold. *J. Biomed. Mater. Res., Part A* **2007**, *83A* (4), 1039−1046.
(29) Bertoni, F.; Barbani, N.; Giusti, P.; Ciardelli, G. Transglutaminase Reactivity with Gelatine: Perspective Applications in Tissue Engineering. *Biotechnol. Lett.* **2006**, *28* (10), 697−702.
(30) Irvine, S. A.; Agrawal, A.; Lee, B. H.; Chua, H. Y.; Low, K. Y.; Lau, B. C.; Machluf, M.; Venkatraman, S. Printing Cell-Laden Gelatin Constructs by Free-Form Fabrication and Enzymatic Protein Crosslinking. *Biomed. Microdevices* **2015**, *17* (1), 16.
(31) Rodriguez, G. M.; Trueb, D.; Köser, J.; Schoelkopf, J.; Gullo, M. An Origami like 3D Patterned Cellulose-Based Scaffold for Bioengineering Cardiovascular Applications. *Cellulose* **2023**, *30*, 10401.
(32) Radisic, M.; Marsano, A.; Maidhof, R.; Wang, Y.; Vunjak-Novakovic, G. Cardiac Tissue Engineering Using Perfusion Bioreactor Systems. *Nat. Protoc.* **2008**, *3* (4), 719−738.
(33) Pisanu, A.; Reid, G.; Fusco, D.; Sileo, A.; Diaz, D. R.; Tarhini, H.; Putame, G.; Massai, D.; Isu, G.; Marsano, A. Bizonal Cardiac Engineered Tissues with Differential Maturation Features in a Mid-Throughput Multimodal Bioreactor. *iScience* **2022**, *25* (5), 104297.
(34) Cholewinski, E.; Dietrich, M.; Flanagan, T. C.; Schmitz-Rode, T.; Jockenhoevel, S. Tranexamic Acid—An Alternative to Aprotinin in Fibrin-Based Cardiovascular Tissue Engineering. *Tissue Eng. Part A* **2009**, *15* (11), 3645−3653.
(35) Sacchi, V.; Mittermayr, R.; Hartinger, J.; Martino, M. M.; Lorentz, K. M.; Wolbank, S.; Hofmann, A.; Largo, R. A.; Marschall, J. S.; Groppa, E.; Gianni-Barrera, R.; Ehrbar, M.; Hubbell, J. A.; Redl, H.; Banfi, A. Long-Lasting Fibrin Matrices Ensure Stable and Functional Angiogenesis by Highly Tunable, Sustained Delivery of Recombinant VEGF164. *Proc. Natl. Acad. Sci. U. S. A.* **2014**, *111* (19), 6952−6957.
(36) Dunn, G. A.; Heath, J. P. A New Hypothesis of Contact Guidance in Tissue Cells. *Exp. Cell Res.* **1976**, *101* (1), 1−14.
(37) Navaei, A.; Moore, N.; T. Sullivan, R.; Truong, D.; Migrino, R. Q.; Nikkhah, M. Electrically Conductive Hydrogel-Based Micro-Topographies for the Development of Organized Cardiac Tissues. *RSC Adv.* **2017**, *7* (6), 3302−3312.
(38) Lemme, M.; Ulmer, B. M.; Lemoine, M. D.; Zech, A. T. L.; Flenner, F.; Ravens, U.; Reichenspurner, H.; Rol-Garcia, M.; Smith, G.; Hansen, A.; Christ, T.; Eschenhagen, T. Atrial-like Engineered Heart Tissue: An In Vitro Model of the Human Atrium. *Stem Cell Rep.* **2018**, *11* (6), 1378−1390.
(39) Isu, G.; Robles Diaz, D.; Grussenmeyer, T.; Gaudiello, E.; Eckstein, F.; Brink, M.; Marsano, A. Fatty Acid-Based Monolayer Culture to Promote *in Vitro* Neonatal Rat Cardiomyocyte Maturation. *Biochim. Biophys. Acta, Mol. Cell Res.* **2020**, *1867* (3), 118561.
(40) Gabetti, S.; Sileo, A.; Montrone, F.; Putame, G.; Audenino, A. L.; Marsano, A.; Massai, D. Versatile Electrical Stimulator for Cardiac Tissue Engineering—Investigation of Charge-Balanced Monophasic and Biphasic Electrical Stimulations. *Front. Bioeng. Biotechnol.* **2023**, *10*, 1031183.
(41) Helmrich, U.; Di Maggio, N.; Güven, S.; Groppa, E.; Melly, L.; Largo, R. D.; Heberer, M.; Martin, I.; Scherberich, A.; Banfi, A. Osteogenic Graft Vascularization and Bone Resorption by VEGF-Expressing Human Mesenchymal Progenitors. *Biomaterials* **2013**, *34* (21), 5025−5035.
(42) Marsano, A.; Conficconi, C.; Lemme, M.; Occhetta, P.; Gaudiello, E.; Votta, E.; Cerino, G.; Redaelli, A.; Rasponi, M. Beating Heart on a Chip: A Novel Microfluidic Platform to Generate Functional 3D Cardiac Microtissues. *Lab Chip* **2016**, *16* (3), 599−610.
(43) McDevitt, T. C.; Angello, J. C.; Whitney, M. L.; Reinecke, H.; Hauschka, S. D.; Murry, C. E.; Stayton, P. S. In Vitro Generation of Differentiated Cardiac Myofibers on Micropatterned Laminin Surfaces. *J. Biomed. Mater. Res.* **2002**, *60* (3), 472−479.

https://doi.org/10.1021/acsbiomaterials.4c01594
ACS Biomater. Sci. Eng. 2025, 11, 1583−1597